

## Critical behavior at electronically driven structural transitions in anisotropic metals\*

P. M. Horn<sup>†</sup> and D. Guidotti

*The Department of Physics and The James Franck Institute, The University of Chicago, Chicago, Illinois 60637*

(Received 30 August 1976; revised manuscript received 10 November 1976)

We present the results of high-precision electrical-resistivity measurements in the vicinity of the three-dimensional structural transitions in TTF-TCNQ (tetrathiafulvalene-tetracyanoquinodimethane) and TSeF-TCNQ (tetraselenafulvalene-tetracyanoquinodimethane). We find a sharp negative divergence in the derivative of the resistivity  $(1/\rho)(d\rho/dT)$ , which is similar in form to the resistive anomalies observed in metallic antiferromagnets and suggests the existence of a second-order phase transition at about  $T_c \simeq 53$  and 29 K in TTF-TCNQ and TSeF-TCNQ, respectively. A systematic comparison between theory and experiment including a critical-exponent analysis of the resistive anomaly has led to the following conclusions: (i) For  $T - T_c \rightarrow 0^+$ , the resistivity is most probably dominated by an enhancement in the electron-phonon scattering associated with the critical fluctuations in the  $q = 2k_F$  phonons. (ii) For  $T - T_c \rightarrow 0^-$ , the resistivity appears to be dominated by the opening of an electronic gap at the Fermi surface. (iii) The overall structure of the resistive anomaly including the temperature dependence of  $\rho$  in the high-temperature phase suggests strongly that the fluctuation growth in these materials is rather isotropic and that for  $T$  above  $T_c$  there does not exist a large one-dimensional correlation length.

### I. INTRODUCTION

There has been considerable recent interest in electronically driven structural transitions in metals with large one- and two-dimensional anisotropy.<sup>1-10</sup> In the one-dimensional systems, much of the recent interest has centered around the possibility of having large regions of temperature where the physical properties of the system are dominated by the growth of one-dimensional fluctuations along the conducting axis.<sup>11-14</sup> The physical origin of these fluctuations can be understood by considering a hypothetical one-dimensional metal. Peierls<sup>15</sup> has shown that at temperatures below some mean-field scale energy  $T_c^{\text{MF}}$ , a one-dimensional metal is energetically unstable with respect to a lattice (Peierls) distortion which induces a gap at the Fermi surface and transforms the metal into a semiconductor. However, while it is energetically favorable when  $T < T_c^{\text{MF}}$  for the system to distort, it will do so only when the free energy is lower in the semiconducting phase than in the metallic phase. For a one-dimensional system this occurs only at  $T = 0$ .<sup>16</sup> Therefore for  $0 < T \ll T_c^{\text{MF}}$  we expect large fluctuations and no long-range order.

Now consider a real three-dimensional material with one-dimensional anisotropy in the conductivity. To be specific we restrict our discussion to a system of weakly coupled one-dimensional chains. If the coupling between the chains is sufficiently weak, the arguments are similar to those given for the one-dimensional material. For  $T < T_c^{\text{MF}}$  (where  $T_c^{\text{MF}}$  is the scale energy of an isolated chain) the one-dimensional fluctuations grow and apparently diverge only at  $T = 0$ . However,

when  $T$  becomes sufficiently small, the interactions between the chains may no longer be considered a weak contribution to the free energy, and the one-dimensional fluctuations couple to drive a three-dimensional phase transition (at  $T = T_c$ ).

The organic linear chain complex TTF-TCNQ and its isostructural analogs have been the prototypical systems for studying the physical properties of electronically driven one-dimensional structural fluctuations. Their primary advantage over, for example, the metal chain complexes<sup>17,18</sup> is that the former contain no intrinsic structural disorder and as a consequence have, in general, a well-defined three-dimensional phase transition which is absent in the metal chain complexes.<sup>19</sup> In TTF-TCNQ specifically, recent diffuse x-ray studies<sup>1,2</sup> as well as elastic<sup>3</sup> and inelastic<sup>4</sup> neutron scattering experiments have shown that the metal-nonmetal transition is associated with a structural distortion arising from the condensation of a  $q = 2k_F$  phonon. Therefore, while there exists many possible one-dimensional instabilities, it appears that the Peierls-distortion picture is appropriate for TTF-TCNQ. On the other hand, there is as yet little detailed experimental information about the actual character of the fluctuations associated with this distortion and the role they play in determining the bulk properties of these materials.

In this paper we present a detailed examination of the contributions which structural fluctuations make to the electrical resistivity of TTF-TCNQ and TSeF-TCNQ. While the experimental data and theory pertain primarily to the immediate vicinity of the three-dimensional ordering temperature ( $T \simeq T_c$ ), many of the conclusions presented relate

to the larger question of fluctuation behavior in the high-temperature phase ( $T > T_c$ ). In Sec. II we present our experimental techniques and results. In Secs. III and IV we present a simple model calculation for the electrical resistivity of a highly anisotropic metal which includes both the enhancement of the electron-phonon scattering near the three-dimensional ordering temperature and the density-of-states effects arising from the opening of an electronic gap at the Fermi surface. In Sec. V we present a detailed comparison of experiment with theory and any conclusions obtained therein.

## II. EXPERIMENTAL DETAILS AND RESULTS

The samples, for this study, single crystals of TTF-TCNQ and TSeF-TCNQ, were obtained from and characterized by several different laboratories.<sup>20</sup> Typical sample dimensions were 0.2–1.0 cm long, 0.2–0.7 mm wide, and 0.07–0.1 mm thick with the long axis corresponding to the highly conducting crystallographic  $b$  axis. Electrical contact to the crystals was made using 0.018-mm-diam gold wire affixed to the sample surface with silver conducting paint. The contacts were checked and found to be nonrectifying with a typical contact resistance on the order of 5–15  $\Omega$ . The  $b$ -axis conductivity was obtained by wiring the samples in the standard four-probe configuration with contacts nearly equally spaced along the  $b$  axis. The  $a$ -axis conductivity of TTF-TCNQ was measured by placing four approximately equally spaced contacts across the width ( $a$  axis) of one of the wider ( $\sim 2$  mm)  $b$ -axis crystal. Each contact spanned the entire length ( $\sim 5$  mm) of the crystal.

The electrical-resistivity measurements were made using a four-probe ac null technique (at 39 Hz) with a limiting sensitivity of about  $2 \times 10^{-10}$  V and precision of one part in  $10^5$ . The driving current, typically on the order of a few microamperes rms, and the phase sensitive null were obtained using a PAR lock in amplifier. The data in the critical region were taken at a drift rate of 0.4–1.0 K/h while the sample temperature was continuously monitored with a carbon thermistor which had a relative sensitivity of 0.4–1.0 mK and an absolute calibration to about 0.4 K. To insure temperature homogeneity, the sample was mounted on a sapphire substrate which was glued into an oxygen-free copper holder which contained the carbon resistor and other temperature sensors. The sample holder was designed in such a manner that the mounted sample and substrate were completely surrounded by the high-thermal-conductivity copper. The sample holder was then mounted in a copper vacuum can which was main-

tained at a partial pressure of helium exchange gas.

To minimize the possibility of spurious results arising from anomalous current flow patterns, the nested and unnested current-voltage characteristics were measured at both 300 and 77 K.<sup>21</sup> Results were considered significant only if the unnested voltages were less than 5% of their nested counterparts.

Temperature derivatives of the experimental curves were obtained from the primary resistance versus temperature data. A least-squares fit to a linear functional form was made, typically, over five adjacent data points, or over a region 90–200 mK wide. Local values of the derivative at each temperature datum is then obtained by sliding the region of fit over the entire experimental temperature range while analytically computing the derivative from the fitted linear curves.

Experimental results are shown in Figs. 1–4. The overall temperature dependence of the  $b$ -axis conductivity of TTF-TCNQ is shown in Fig. 1. The solid line through the data in Fig. 1 represents a least-squares fit of the high-temperature resistivity to the functional form

$$\rho(T) = \rho_0 + AT^n, \quad (2.1)$$

where  $\rho(T)$  is the  $b$ -axis resistivity and  $\rho_0$ ,  $A$ , and  $n$  are constants. Equation (2.1) was found to be a good representation of the high-temperature resistivity in all of the approximately 20 samples of TTF-TCNQ analyzed in this study.<sup>22</sup> The parameter  $n$  was found to be relatively universal ranging between 2.4 and 2.55 while  $\rho_0$  was found to be extremely sample dependent ranging from  $2\% \lesssim \rho_0/\rho(\text{RT}) \lesssim 15\%$  where  $\rho(\text{RT})$  is the room temperature  $b$ -axis resistivity. Consistent with the sample dependence of  $\rho_0$  we found that the mag-

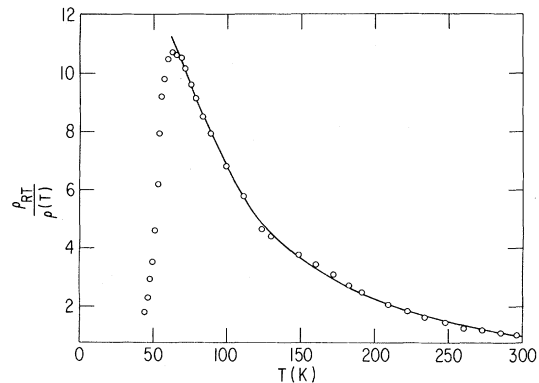


FIG. 1. Temperature dependence of  $b$ -axis conductivity in TTF-TCNQ. The solid line represents a least-square fit to the functional form in Eq. (2.1).

nitude of the peak in the conductivity at  $T = 60$  K was strongly sample dependent with  $\rho(RT)/\rho(60 \text{ K}) \approx 28$  when  $\rho_0/\rho(RT) \approx 2\%$  and  $\rho(RT)/\rho(60 \text{ K}) \approx 6$  when  $\rho_0/\rho(RT) \approx 15\%$ . We will not speculate on the origin of this unusual temperature dependence of the electrical conductivity in TTF-TCNQ, but note that the behavior is similar to that observed in many anisotropic organic conductors<sup>22,23</sup> and is consistent with model calculations for the ideal electron-phonon resistivity in a one-dimensional metal.<sup>24</sup> Many other explanations are also possible.<sup>11,25</sup>

For comparison, the overall temperature dependence of the  $a$ -axis resistivity of TTF-TCNQ was measured and compared with our  $b$ -axis results. We find (data not shown) that if we force the  $a$ -axis data to Eq. (2.1) we obtain  $0.9 \lesssim n \lesssim 1.3$ , with the best-fit value of  $n$  depending strongly on the region of fit. This temperature dependence is in quantitative agreement with the  $a$ -axis resistivity data reported by Cohen *et al.*,<sup>12</sup> and can be considered as a consistency check on our  $a$ -axis data.

We focus in this paper on the critical behavior in the electrical conductivity which occurs at temperatures below the conductivity maximum as illustrated in Figs. 2–4. In Figs. 2 and 4 we display the temperature derivative of the  $b$ -axis resistance of TTF-TCNQ and TSeF-TCNQ, respectively, as a function of temperature. In both cases the divergence is sharply peaked, although the TSeF-TCNQ divergence is comparatively narrower, more symmetric and somewhat sharper. In contrast the critical behavior of  $a$ -axis TTF-TCNQ, shown in Fig. 3, is somewhat weaker in that the temperature derivative of the  $a$ -axis resistance rises above the base line only half as much as the  $b$ -axis divergence. Figure 3 shows a broader, more rounded peak than is obtained with  $b$ -axis TTF-TCNQ, even taking into account the slight variations with different samples. A word should be said about the reproducibility of these results. To the present we have examined the critical behavior of six different samples of TTF-TCNQ; four  $b$ -axis measurements and two  $a$ -axis measurements. All of the samples studied had the qualitative shapes shown in Figs. 2 and 3. Both the rounding of the transition and the position of  $T_c$  were found to be sample dependent with the sharper transitions occurring in the samples with higher transition temperatures. Alternatively, the critical exponents associated with these transitions were found to be sample independent and within the uncertainties quoted in Sec. V.

The sharp divergence in  $dR/d(1/T)$  [or negative divergence in  $R^{-1}(dR/dT)$ ] is similar in form to the resistive anomalies observed at the Néel temperature in metallic antiferromagnetics and occurs in

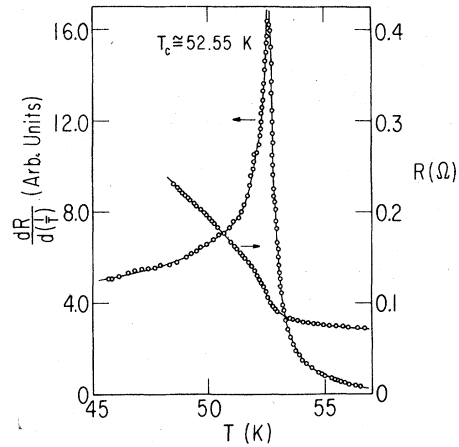


FIG. 2. Detailed behavior of the  $b$ -axis resistance  $R$  of TTF-TCNQ and its derivative  $dR/d(1/T)$  in the vicinity of the critical temperature.

TTF-TCNQ at the same temperature ( $\sim 53$  K) as the observed peak in the specific heat.<sup>7</sup> Furthermore, at about 53 K there is a sharp increase in the intensity of elastically scattered neutrons at the Bragg peaks associated with the crystal structure of the low-temperature phase.<sup>3</sup> These facts suggest the existence of a three-dimensional second-order phase transition at about  $T_c = 53$  K in TTF-TCNQ and by analogy at about  $T_c = 29$  K in TSeF-TCNQ. We are led to conclude that the sharp peaks in the electrical resistivity are manifestations of the critical fluctuations associated with the three-dimensional onset of Peierls order, in which the order parameter (perhaps complex) is the lattice distortion generated by the condensa-

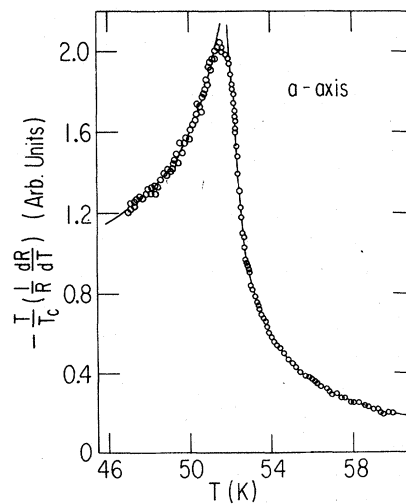


FIG. 3. Behavior of the logarithmic derivative of the  $a$ -axis resistance in TTF-TCNQ near the critical temperature.

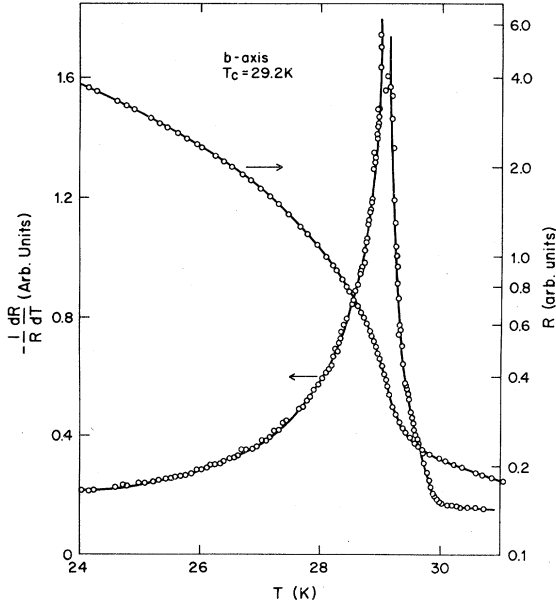


FIG. 4. *b*-axis resistance  $R$  of TSeF-TCNQ and its logarithmic derivative in the vicinity of the critical temperature  $T_c \cong 29.2^\circ\text{K}$ .

tion of a  $q = 2k_F$  phonon.<sup>19</sup> In the analysis that follows we will attempt to explain these critical divergences in the derivative of the electrical resistivity in terms of the above model for the phase transitions in TTF-TCNQ and TSeF-TCNQ. A detailed critical exponent analysis of the electrical resistivity will be presented in Sec. V after the presentation of a model calculation of the critical behavior in the electrical resistivity.

### III. CRITICAL SCATTERING

In this section we outline a simple approximate approach for treating the critical scattering contribution to the electrical resistivity. The motivation for the approximations contained herein lies in the qualitative similarity between the observed resistivity anomalies in the linear chain compounds and those seen in metallic antiferromagnets.<sup>26,27</sup> The approach and approximations can be summarized as follows: The electron-phonon scattering is treated using standard second-order perturbation theory while the anomalous temperature dependence of the electronic response functions are put in by hand using universality arguments near the three-dimensional phase transition. This approach, while being exactly analogous to that taken by Fisher and Langer<sup>28</sup> and others<sup>29-31</sup> to describe resistive anomalies in magnetic metals, is clearly not self-consistent when applied to electronically driven transitions since critical

divergences in the phonon response functions do not arise within the second-order perturbation approximation used to describe the critical scattering. Physically the approximation can be thought of as a scheme for decoupling the electron and phonon systems, treating only scattering of electrons from the critical fluctuations of the phonons while neglecting any collective current carrying effects which could arise in a self-consistent treatment.<sup>32-34</sup>

The diagonal part of the resistivity tensor can be written in the Born approximation as<sup>35</sup>

$$\rho_{\mu\mu} \propto \int d^d k \int d^d q |g_{\vec{k}}|^2 (k_\mu)^2 f(\epsilon_{\vec{q}}) [1 - f(\epsilon_{\vec{k}+\vec{q}})] \times \int d\omega S(\vec{k}, \omega) \delta(\epsilon_{\vec{q}} - \epsilon_{\vec{k}+\vec{q}} - \hbar\omega), \quad (3.1)$$

where  $f$  is a Fermi function,  $g_{\vec{k}}$  is the electron-phonon coupling constant,  $\mu$  is a direction index, and  $S(\vec{k}, \omega)$  is the dynamic form factor defined by

$$S(\vec{k}, \tau) = \int_{-\infty}^{\infty} \frac{d\omega}{2\pi} S(\vec{k}, \omega) e^{i\omega\tau} \quad (3.2)$$

and

$$S(\vec{k}, \tau) = \langle \rho_{\vec{k}}(\tau) \rho_{\vec{k}}^\dagger(0) \rangle, \quad (3.3)$$

where  $\rho_{\vec{k}}$  is the Fourier transform of the electron density. We specifically consider the situation where  $S(\vec{k} = 2\vec{k}_F, \tau = 0)$  diverges at  $T \rightarrow T_c$ , where  $T_c$  is the three-dimensional ordering temperature. For  $T$  near  $T_c$ , the usual critical-slowing-down argument can be made<sup>28</sup> by noting that  $d\rho_{\mu\mu}/dT$  is dominated by  $\vec{k} = 2\vec{k}_F$  scattering and hence by  $dS(2\vec{k}_F, \omega)/dT$ . However  $S(2\vec{k}_F, \omega)$  is sharply peaked at  $\omega = 0$  and therefore the frequency integral is not limited by  $\delta(\epsilon_{\vec{q}} - \epsilon_{\vec{k}+\vec{q}} - \hbar\omega)$  for any finite  $T_c$ . We obtain therefore

$$\frac{d\rho_{\mu\mu}}{dT} \propto \int d^d k \int d^d q |g_{\vec{k}}|^2 (k_\mu)^2 f(\epsilon_{\vec{q}}) [1 - f(\epsilon_{\vec{k}+\vec{q}})] \times \frac{dS(\vec{k})}{dT} \delta(\epsilon_{\vec{q}} - \epsilon_{\vec{k}+\vec{q}}), \quad (3.4)$$

where  $S(\vec{k})$  is the static or equal-time density-density response function defined by

$$S(\vec{k}) \equiv S(\vec{k}, \tau = 0) = \langle \rho_{\vec{k}} \rho_{\vec{k}}^\dagger \rangle. \quad (3.5)$$

A similar argument can be made for the  $k$  integral. As  $T \rightarrow T_c$ ,  $dS(\vec{k})/dT$  becomes sharply peaked at  $\vec{k} = 2\vec{k}_F$  and hence the  $\delta$  function in Eq. (3.4) does not limit the  $k$  integration. The validity of this approximation will be discussed subsequently. Assuming  $|g_{\vec{k}}|^2$  is a weak function of  $\vec{k}$ , for  $\vec{k}$  near  $2\vec{k}_F$  we obtain

$$\frac{d\rho_{\mu\mu}}{dT} \propto |g_{2\vec{k}_F}|^2 \int d^d k' \frac{[(2k_F)_\mu + (k')_\mu]^2}{|2\vec{k}_F + \vec{k}'|} \times \frac{dS(2\vec{k}_F + \vec{k}')}{dT}. \quad (3.6)$$

Defining the order parameter  $\Delta_{\vec{k}} = \rho_{2\vec{k}_F + \vec{k}'}$  and the order parameter-order parameter correlation function

$$\chi(\vec{k}) = \beta \langle |\Delta_{\vec{k}}|^2 \rangle, \quad (3.7)$$

where  $\beta = 1/k_B T$ , Eq. (3.6) becomes

$$\frac{d\rho_{\mu\mu}}{dT} \propto \frac{|g_{2\vec{k}_F}|^2}{\beta} \int d^d k' \frac{[(2k_F)_\mu + (k')_\mu]^2}{|2\vec{k}_F + \vec{k}'|} \frac{d\chi(\vec{k}')}{dT}. \quad (3.8)$$

For  $T$  near  $T_c$ , the dominant contribution to the divergence in Eq. (3.8) comes from the  $(2k_F)_\mu^2$  term. Thus

$$\begin{aligned} \frac{d\rho_{\mu\mu}}{dT} &\propto \frac{|g_{2\vec{k}_F}|^2 (2k_F)_\mu^2}{\beta} \int d^d k' \frac{1}{|2\vec{k}_F + \vec{k}'|} \frac{d\chi(\vec{k}')}{dT} \\ &\simeq \frac{(2k_F)_\mu^2}{|2\vec{k}_F|} \frac{|g_{2\vec{k}_F}|}{\beta} \int \frac{d\chi(\vec{k}')}{dT} d^d k'. \end{aligned} \quad (3.9)$$

The dimensionality  $d$  in Eq. (3.9) is *not* the dimensionality of the fluctuations (which we assume to be "three" for  $T$  near  $T_c$ ), but rather the dimensionality determined by the allowed final states for scattering. If for example the condition is limited to chains then  $d=1$ , while if the scattering is in planes  $d=2$ , etc. The critical behavior of  $\rho$  is simply determined from Eq. (3.9) by power counting. The results are

$$d=1, \quad \frac{d\rho}{dT} \sim t^{-(1+\nu+\eta\nu)} \sim t^{-1.5}, \quad (3.10a)$$

$$d=2, \quad \frac{d\rho}{dT} \sim t^{-(1+\eta\nu)} \sim t^{-1.0}, \quad (3.10b)$$

$$d=3, \quad \frac{d\rho}{dT} \sim t^{-(1+\eta\nu-\nu)} \sim t^{-0.5}, \quad (3.10c)$$

where  $t = (T - T_c)/T_c$ ,  $\nu$  is the critical exponent for the correlation length and  $\eta$  is the exponent for the momentum dependence of  $\chi(k)$  at  $T = T_c$ . To illustrate the magnitude of the numbers involved, we have included on the right in Eq. (3.10) the mean-field values for the predicted exponents (i.e.,  $\eta = 0$ ,  $\nu = 0.5$ ). Note that the critical part of  $d\rho/dT$  depends on the direction  $\mu$  only insofar as  $d$  depends on  $\mu$ . Equation (3.10c) is just the Suzuki-Mori<sup>29</sup> result for the temperature dependence of  $d\rho/dT$  in metallic antiferromagnets above the Néel temperature.

We now turn to the question of the validity of the approximations which allowed us to write Eq. (3.4) as Eq. (3.6). The  $\delta$  function in Eq. (3.4) can be

neglected when the peak in  $dS(\vec{k})/dT$  about  $\vec{k} = 2\vec{k}_F$  is much narrower than the finite temperature smearing of the Fermi surface in  $\vec{k}$  space. In the extreme incommensurate limit (i.e.,  $E_F = \hbar^2 k_F^2/2m$ ) this requirement reduces to

$$\frac{\xi_{||}(T)}{b} \gg \left( \frac{E_F}{2k_B T} \right)^{1/2}, \quad (3.11)$$

where  $b$  is the  $b$ -axis lattice constant,  $\xi_{||}(T)$  is the longitudinal coherence length, and  $E_F$  is the Fermi energy. For the organic materials under consideration,  $(E_F/2k_B T_c)^{1/2} \lesssim 6$ ,<sup>7</sup> and Eq. (3.11) is easily satisfied for  $T$  near  $T_c$ .

The above formalism is appropriate only for  $T > T_c$ . For  $T < T_c$  one must subtract off the contribution from the onset of long-range order [i.e.,  $\langle \Delta(\vec{x}) \rangle \neq 0$ ] and the scattering contribution to  $\rho$  decreases as  $T$  decreases below  $T_c$ .<sup>29</sup> Since the resistivity is increasing as  $T$  decreases below  $T_c$  (see Fig. 1), it must be dominated for  $T < T_c$  by the opening of an electronic gap at the Fermi surface rather than by critical scattering. We now treat this effect.

#### IV. THE ELECTRONIC GAP

In Sec. III we estimated the contribution to  $\rho$  arising from electrons scattering from order parameter fluctuations. A tacit assumption of Sec. III was that the number of conduction electrons remained fixed. In this section we estimate the contribution to  $\rho$  arising from the opening of a fluctuating gap in the conduction band. As in Sec. III, the model developed will represent the simplest one-electron picture possible.

Recall that the longitudinal correlation length  $\xi_{||}$  represents the distance scale for longitudinal changes in the order parameter  $\Delta(\vec{x})$ . When  $\xi_{||} \gg \lambda$  where  $\lambda$  is the mean free path, the conduction electrons (or holes) scatter many times in a region where the order parameter (and hence the electronic gap) is relatively constant. It is then possible to define a local value,  $\rho(\Delta(\vec{x}))$ , of the resistivity  $\rho$ . If the one-dimensional anisotropy of the conduction is large, the conduction electrons cannot skirt regions where the local gap is large. In this limit the local resistivities add in series and hence

$$\rho = \langle \rho(\Delta(\vec{x})) \rangle, \quad (4.1)$$

where  $\langle \rangle$  represents the usual statistical average defined by

$$\rho = \frac{1}{z} \int \delta\Delta(x) \rho(\Delta(\vec{x})) \exp\left(\frac{-F}{k_B T}\right), \quad (4.2)$$

where  $z$  is the partition function,  $F$  is the Ginzburg-Landau free-energy functional, and  $\int \delta\Delta(x)$

represents a functional integral over all order-parameter configurations.<sup>36</sup> For  $F$  we choose a form characteristic of weakly coupled chains. For example, one might use<sup>37</sup>

$$F = \sum_i \int_0^L dx [r_0 |\Delta_i(x)|^2 + u |\Delta_i(x)|^4 + C_{\parallel} |\partial_x \Delta(x)|^2] + 2 \sum_{i \neq j} C_{\perp} \int_0^L |\Delta_i \Delta_j| dx, \quad (4.3)$$

where  $i, j$  are chain indices,  $C_{\parallel}$  and  $C_{\perp}$  are the intra- and interchain coupling constants, and  $r_0 = r'_0(T/T_c^{\text{MF}} - 1)$ , where  $r'_0$  and  $u$  are constants and  $T_c^{\text{MF}}$  is the mean-field scale energy of an individual chain.

In order to evaluate Eq. (4.2) one needs a form for the local resistivity  $\rho(\Delta)$ . Since the electrons scatter many times in a region where  $\Delta$  is uniform,  $\rho(\Delta)$  can be obtained in a simple one-electron band picture. The excitation spectrum in the presence of a complex gap  $\Delta_k$  is given by<sup>32</sup>

$$E_k = (\epsilon_k^2 + |\Delta_k|^2)^{1/2}, \quad (4.4)$$

where  $\epsilon_k$  is the unperturbed free-electron band structure. The conductivity is then obtained from

$$\sigma[\Delta] = \frac{1}{\rho[\Delta]} = \int \sigma(E) \frac{-\partial f}{\partial E} dE, \quad (4.5)$$

where  $\sigma(E)$  is the energy-dependent conductivity in the band  $E_k$  and  $f$  is the Fermi distribution function. Assuming a simple cosine band for  $\epsilon_k$ , we obtain

$$\frac{1}{\rho(\Delta)} = \frac{1}{\rho_0} \frac{1}{1 + (|\Delta|/k_B T)^2} \quad (|\Delta| < k_B T), \quad (4.6a)$$

$$\frac{1}{\rho(\Delta)} = \frac{1}{\rho_0} \frac{1}{1 + e^{|\Delta|/k_B T}} \quad (|\Delta| > k_B T). \quad (4.6b)$$

The resistivity  $\rho$  becomes

$$\rho = \rho_0 [1 + \langle |\Delta|^2 \rangle / (k_B T)^2] \quad (\langle |\Delta| \rangle < k_B T), \quad (4.7a)$$

$$\rho = \rho_0 [1 + \langle e^{|\Delta|/k_B T} \rangle] \quad (\langle |\Delta| \rangle > k_B T). \quad (4.7b)$$

$\rho_0$  contains the scattering contribution estimated in Sec. III and  $\Delta\rho \equiv (\rho - \rho_0)/\rho_0$  represents the contribution to  $\rho$  from the decrease in the number of conduction electrons. While it is not possible to analytically evaluate the functional integral in Eq. (4.7), the temperature dependence of  $\Delta\rho$  can be determined in various limiting regions. To be specific, let us first assume that we are dealing with a highly anisotropic material with  $T_c \ll T_c^{\text{MF}}$ , where  $T_c$  is the three-dimensional ordering temperature. We distinguish four temperature regions: (a)  $T \gg T_c^{\text{MF}}$ , (b)  $T \cong T_c^{\text{MF}}$ , (c)  $T_c < T \ll T_c^{\text{MF}}$ , and (d)  $T < T_c$ .

In *region (a)* the temperature dependence of  $\Delta\rho$

is obtained from (4.7a)

$$\Delta\rho = \frac{\langle |\Delta|^2 \rangle}{(k_B T)^2} = \frac{1}{(k_B T)^2} \int_0^{\Lambda} \chi(k) d^3 k, \quad (4.8)$$

where  $\chi(k)$  is the order-parameter susceptibility defined in Sec. III and  $\Lambda$  is the upper momentum cutoff. For  $T \gg T_c^{\text{MF}}$  a Gaussian approximation for  $\chi(k)$  is sufficient and  $\langle |\Delta|^2 \rangle \sim \xi_{\parallel}^2(T) \sim (T - T_c^{\text{MF}})^{-1}$  for  $\xi_{\parallel}(T) \ll \Lambda$  and  $\langle |\Delta|^2 \rangle \sim \Lambda - \frac{1}{2} \pi \xi_{\parallel}^{-1}(T)$  for  $\xi_{\parallel}(T) > \Lambda$ .

In *region (b)* the temperature dependence is complicated, but can be approximated by retaining Eq. (4.8) while using  $\langle |\Delta|^2 \rangle \sim \Lambda - \frac{1}{2} \pi \xi_{\parallel}^{-1}(T)$  with  $\xi_{\parallel}^{-1}(T) \sim T/T_c^{\text{MF}}$ .<sup>38</sup>

When  $T$  becomes much less than  $T_c^{\text{MF}}$  as in *region (c)*,  $F$  becomes highly nonlinear and  $\langle |\Delta| \rangle$  becomes greater than  $k_B T$ . In this region  $\Delta\rho$  becomes

$$\Delta\rho = \langle e^{|\Delta(x)|/k_B T} \rangle = \exp \left( \frac{\langle |\Delta| \rangle}{k_B T} + \frac{\langle |\Delta|^2 \rangle - \langle |\Delta| \rangle^2}{2(k_B T)^2} + \dots \right). \quad (4.9)$$

To a good approximation  $\langle |\Delta|^2 \rangle = \langle |\Delta| \rangle^2$  and the cumulant expansion in Eq. (4.9) can be truncated after the first term. The dominant contribution to  $\langle |\Delta| \rangle$  comes from values of  $\Delta$  near the minimum in  $F$ . However, the value of  $\Delta$  which minimizes  $F$  is just  $\Delta^{\text{MF}} = \Delta_0 [(T_c^{\text{MF}} - T)/T_c^{\text{MF}}]$ .

Hence

$$\Delta\rho \cong e^{\Delta^{\text{MF}}/k_B T} \quad (4.10)$$

and the resistivity becomes activated. The range of validity of Eq. (4.10) will be discussed in Sec. V.

Finally, as  $T$  passes below  $T_c$  into *region (d)* there is no anomalous contribution to  $\Delta\rho$  near  $T_c$ . In this region  $\langle |\Delta| \rangle \cong \langle \Delta \rangle \cong \Delta^{\text{MF}} \cong \Delta_0$ . Hence

$$\Delta\rho \cong e^{\Delta_0/k_B T}. \quad (4.11)$$

These results are to be contrasted with the behavior of a material in which the fluctuations grow in an isotropic manner such that  $T_c \lesssim T_c^{\text{MF}}$ . For such a material, the temperature dependence of  $\Delta\rho$  can be obtained from Eq. (4.7a) except below the three-dimensional ordering ( $T < T_c$ ), when  $\langle \Delta \rangle > k_B T$ , Eq. (4.7b) must be used. We obtain

$$\Delta\rho \cong \left. \begin{aligned} &\langle |\Delta|^2 \rangle / k_B T, \\ &\langle |\Delta|^2 \rangle \sim \xi^2 \sim (T - T_c^{\text{MF}})^{-1} \end{aligned} \right\} T \gg T_c^{\text{MF}} \quad (4.12)$$

and

$$\Delta\rho \cong \left. \begin{aligned} &\langle |\Delta|^2 \rangle / k_B T, \\ &\langle |\Delta|^2 \rangle \sim |(T - T_c)/T_c|^{1-\alpha} \equiv |t|^{1-\alpha} \end{aligned} \right\} T \cong T_c, \quad (4.13)$$

where  $\alpha$  is the specific heat exponent and

$$\Delta\rho \cong e^{\langle\Delta\rangle/k_B T}, \left\{ \begin{array}{l} T < T_c \\ \langle\Delta\rangle \sim (-t)^\beta \end{array} \right\} \left\{ \begin{array}{l} T < T_c \\ \langle\Delta\rangle > k_B T \end{array} \right\}, \quad (4.14)$$

where  $\beta$  is the critical exponent for the onset of long-range order.

We should point out that since the temperature dependence of  $\rho$  presented above arises from the loss of conduction electrons with  $\rho_0 = \text{const}$ , it should also reflect the temperature dependence of the magnetic susceptibility  $\chi$ . Thus  $\chi = \chi_0 / (1 + \Delta\rho)$  where  $\chi_0$  is the Pauli susceptibility. The linearity of  $\chi$  with  $1/\xi_{||}(T)$  for  $T \gtrsim T_c^{\text{MF}}$  [Eq. (4.7) and following discussion] was first pointed out by Lee, Rice, and Anderson,<sup>34</sup> but as we show above, this linearity does not hold for  $T \ll T_c^{\text{MF}}$  where the electronic contribution to the susceptibility is more nearly activated.

## V. RESULTS AND DISCUSSION

We now turn to a comparison between theory and experiment for the electrical resistivity of TTF-TCNQ and TSeF-TCNQ. First note that neither  $\rho$  nor<sup>39</sup>  $\chi$  is activated in these materials for  $T > T_c$  as would be suggested by Eq. (4.10). Furthermore, there is a sharp specific-heat anomaly in TTF-TCNQ at  $T = T_c$ .<sup>7</sup> These features suggest that the fluctuation growth in these materials is rather isotropic and that for  $T > T_c$  there does not exist a large one-dimensional correlation length along the chains. It may be argued that the absence of an activated resistivity is indicative of collective current carrying effects<sup>13</sup> which have been omitted in the above calculations. As we will show below, the critical behavior of the resistivity argues against this picture. Furthermore, if  $\xi_{||}(T) \gg \xi_{||}(0)$  [where  $\xi_{||}(0)$  is the zero-temperature correlation length], the absence of an activated susceptibility would be much more difficult to explain and would require abandoning the entire idea of a Peierls distortion in TTF-TCNQ.<sup>40</sup>

Let us quantify the above arguments. The validity of Eq. (4.10) requires that  $T/T_c^{\text{MF}} \lesssim 1 - \Delta t$ ,<sup>41</sup> where  $\Delta t$  is a dimensionless parameter which is a measure of the temperature width of the one dimensional ordering. Therefore, the existence in TTF-TCNQ of a large specific-heat peak<sup>42</sup> and the absence of an activated magnetic susceptibility requires that  $T_c$  be in the vicinity of the smeared one-dimensional ordering below  $T_c^{\text{MF}}$  or

$$T_c/T_c^{\text{MF}} \gtrsim 1 - \Delta t. \quad (5.1)$$

$\Delta t$  can be related to the Landau coefficients in Eq. (4.3)<sup>41</sup>;

$$\Delta t = 2 \left( \frac{uk_B T_c^{\text{MF}}}{v_0'^2} \right)^{2/3} \cong 0.258 \left( \frac{e^{1/2}}{N(0)E_F} \right)^{2/3}, \quad (5.2)$$

where  $\lambda$  is the dimensionless electron-phonon coupling constant at  $q = 2k_F$ ,  $E_F$  is the Fermi energy, and  $N(0)$  is the density of states at the Fermi energy. The last equality in Eq. (5.2) is obtained following Allender, Bray, and Bardeen who relate the Landau coefficients to microscopic parameters via a mean field decoupling of the Peierls-Frohlich Hamiltonian.<sup>32</sup> Inserting reasonable experimental numbers [ $N(0) \cong 3 \text{ eV}^{-1}$ ,<sup>7</sup>  $E_F \cong 0.1 \text{ eV}$ ,<sup>43</sup> and<sup>25,44</sup>  $0.2 \leq \lambda \leq 1$ ] into Eq. (5.2) one immediately finds that  $\Delta t$  can be of order unity and the onset of one-dimensional ordering occurs extremely slowly. Therefore, one cannot expect in these materials a large one-dimensional correlation length for  $T > T_c$ .

We should mention that Horovitz, Gutfreund, and Weger<sup>45</sup> have concluded that  $T_c \cong T_c^{\text{MF}}$  by comparing the magnitude of the specific-heat singularity to a model which includes fluctuations in a Hartree-Fock approximation. We show above however that while the data is consistent with  $T_c \lesssim T_c^{\text{MF}}$ , it is also consistent with  $T_c \ll T_c^{\text{MF}}$  as long as  $(\Delta t)T_c^{\text{MF}} \gtrsim T_c^{\text{MF}} - T_c$ .

We now turn to a discussion of the critical behavior in the electrical resistivity. The arguments given above suggest that in TTF-TCNQ, and by analogy in TSeF-TCNQ, the one dimensional order along the chains is not well developed for  $T \gtrsim T_c$  and consequently the critical behavior in the electrical resistivity is given by Eqs. (4.13), (4.14), and (3.10). A critical exponent analysis of our experimental results is shown in Figs. 5-7. Because of the pronounced temperature dependence for  $T > T_c$  of the  $b$ -axis resistivity in TTF-TCNQ, a background constant was subtracted from  $R^{-1} dR/dT$  to obtain the critical contribution to the resistivity. The background value  $B$  of  $(1/R) dR/dT$

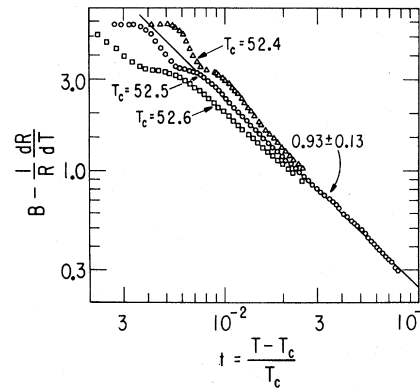


FIG. 5. Critical exponent of  $dR/dT$  for  $T > T_c$  in the  $b$ -axis resistance of TTF-TCNQ. The subtracted background,  $B = R^{-1}(dR/dT)|_{75 \text{ K}} = 0.14$ , is explained in the text.

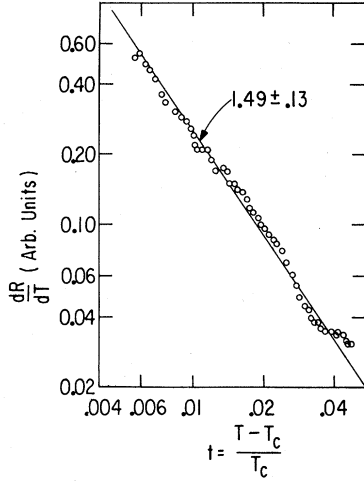


FIG. 6. Critical exponent of  $dR/dT$  above  $T_c$  in the  $b$ -axis resistance TSeF-TCNQ.

$dT$  was chosen to obtain a straight line on the critical-exponent plot in Fig. 5 and has a value  $B = (R^{-1} dR/dT)|_{T=75 \text{ K}}$ . From Fig. 5 we obtain the asymptotic critical behavior  $(1/R)(dR/dT) \sim t^{-0.93 \pm 0.13}$  or  $dR/dT \sim t^{-1.09 \pm 0.15}$  (curve not shown). The uncertainty in the critical exponents reflects the scatter in the experimental data and the uncertainty in both  $T_c$  and the background constant  $B$ . The critical behavior of the  $b$ -axis resistivity of TSeF-TCNQ and of the  $a$ -axis resistivity in TTF-TCNQ is shown in Figs. 6 and 7. In both of these measurements the background temperature dependence of the resistivity for  $T > T_c$  was so weak that the critical behavior was obtained without the subtraction of a background constant. The results are for TSeF-TCNQ,  $b$ -axis  $dR/dT \sim t^{-1.49 \pm 0.13}$ ; and for TTF-TCNQ,  $a$ -axis  $dR/dT \sim t^{-1.04 \pm 0.17}$ .

To compare experiment with theory we note that

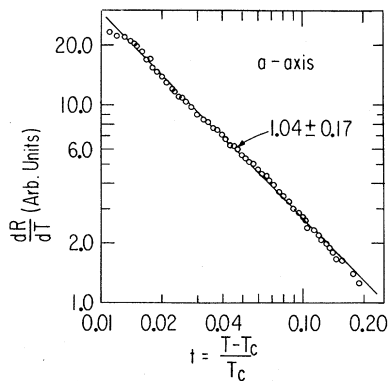


FIG. 7. Critical exponent of  $dR/dT$  above  $T_c$ , in the  $a$ -axis resistance of TTF-TCNQ.

as  $T - T_c \rightarrow 0^+$  the derivative of the resistivity should be dominated by the exponents in Eq. (3.10) since these are larger than the specific-heat-like divergence predicted in Eq. (4.13). The choice of  $d$  in Eq. (3.10) is more complicated, however. One expects that longitudinal ( $b$ -axis) resistivity measurements in highly anisotropic linear chain compounds would be described by  $d=1$  in Eq. (3.10) and  $dR/dT \sim t^{-(1+\eta\nu+\nu)} \cong t^{-1.5}$ . For measurements transverse to the conducting chains the electrons have the entire three-dimensional  $k$  space available to scatter into and if the conduction is large enough to be described with a band-like picture, we expect  $d=3$  and  $dR/dT \sim t^{-1+\eta\nu+\nu} \cong t^{-0.5}$ . Note however that the predicted divergence in the longitudinal resistivity ( $d=1$ ) is stronger than the predicted divergence in the transverse resistivity ( $d=3$ ). Therefore as  $T \rightarrow T_c$ , the resistivity should eventually become isotropic with a divergent behavior in all directions given by Eq. (3.10c). The position in reduced temperature  $t$  of the predicted crossover to an isotropic resistivity depends in part on the magnitude of the anisotropy in the high-temperature conductivity, and the ability to achieve such a crossover in a given experimental system depends on the temperature size of the inhomogeneity rounding of the transition. For TTF-TCNQ the anisotropy in the resistivity is quite large even at  $T \cong T_c$  [ $\rho_a(T \cong T_c)/\rho_b(T \cong T_c) \cong 1000$ ]<sup>12, 21</sup> and the crossover to an isotropic resistivity is never achieved. Therefore in TTF-TCNQ (and by analogy in TSeF-TCNQ) we conclude that the  $b$ -axis resistivity should be described by Eq. (3.10a).

The agreement of these predictions with the experimental results given above is mixed. In TSeF-TCNQ, the  $b$ -axis resistivity does indeed have the critical divergence predicted by Eq. (3.10a). It is our feeling that this agreement is more than fortuitous. On the other hand, the critical behavior of both the  $a$  and the  $b$  axis of TTF-TCNQ appears to be described by Eq. (3.10b) for  $d=2$ . The striking feature of this result is not the magnitude, but rather the equality of the  $a$ - and  $b$ -axis resistivity exponents. The fact that the magnitude of these exponents is given by Eq. (3.10b) could quite possibly be fortuitous, but the equality of these exponents is quite surprising given the fact that the mean free path for  $a$ -axis conduction is much smaller than a lattice constant making a bandlike picture inappropriate to describe the electrical transport.

There are two important features related to the equality of these exponents which should be mentioned. The first of these regards the mechanism dominating the electrical conduction in the high-temperature phase. If, as has been suggested,



the conductivity for  $T > T_c$  is dominated by collective Peierls-Frohlich fluctuations,<sup>11,13</sup> then quite apart from the model given in Sec. III, the critical behavior in the conductivity would arise from three-dimensional pinning of the collective mode. Such a model is inconsistent with the equality of the  $a$ - and  $b$ -axis critical exponents since the collective mode can only propagate along the highly conducting  $b$  axis. Second we should mention that the equality of these exponents is in qualitative agreement with the percolative model of the metal-semiconductor transition suggested by Phillips.<sup>46</sup> This is not to say that the domain model of TTF-TCNQ is quantitatively correct, but merely that it is consistent with this one feature of the experimental data.

We should stress that, as discussed in Sec. II, both the  $b$ - and the  $a$ -axis resistivity measurements on TTF-TCNQ have been reproduced on a variety of samples. We feel that the equality and magnitude of the  $a$ - and  $b$ -axis critical exponents are real, sample-independent results which are not being generated by anomalous current flow patterns or any other experimental artifact.

We discuss now the critical behavior for  $T < T_c$ . The predicted behavior of the resistivity from Eq. (4.13) and Eq. (4.14) for  $T < T_c$  can be summarized as follows<sup>47</sup>:

$$\frac{1}{R} \frac{dR}{dT} \sim (-t)^{\beta-1} \quad (\langle \Delta \rangle \geq k_B T) \quad (5.3)$$

and

$$\frac{1}{R} \frac{dR}{dT} \sim (-t)^{-\alpha} \quad (t \rightarrow 0^-), \quad (5.4)$$

where  $\beta$  is the critical exponent for the onset of long-range order and  $\alpha$  is the specific-heat exponent. Since in mean field theory  $\beta = 0.5$  and  $\alpha = 0$ , the predicted divergence for  $T < T_c$  is much weaker than either the predicted or the observed divergences for  $T > T_c$ . This is in qualitative agreement with our experimental results shown in Figs. 8 and 9.

It is notoriously difficult to obtain good values for either the exponent  $\alpha$  or  $\beta$  from resistivity measurements on metallic antiferromagnets<sup>27</sup> which have the same critical behavior as that predicted in Eqs. (5.3) and (5.4).<sup>29</sup> In the organic complexes studied here, the magnitude of the inhomogeneity rounding of the transition and the resulting uncertainty in the position of  $T_c$  makes determination of  $\alpha$  impossible. One can only conclude that the data is consistent with the small values of  $\alpha$  predicted by well-known theories.<sup>36</sup>

As  $T$  decreases the critical exponents increase as predicted by a crossover from Eq. (5.4) to Eq. (5.3). Because of the limited range of validity of

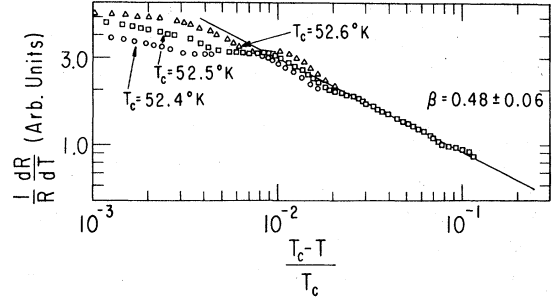


FIG. 8. Critical exponent for  $T < T_c$  of  $(1/R)(dR/dT)$ , where  $R$  is the  $b$ -axis resistance of TTF-TCNQ.

Eq. (5.3) it is difficult to obtain more than a qualitative value for  $\beta$ . We find  $\beta = 0.48 \pm 0.06$  in TTF-TCNQ and  $\beta = 0.24 \pm 0.04$  in TSeF-TCNQ. The quoted uncertainties in  $\beta$  arise primarily from the scatter in the experimental data and represent fitting errors only. The actual uncertainty in these numbers is much greater and arises from fitting the experimental data to Eq. (5.3) outside its region of validity. For example, the small value of  $\beta$  observed in TSeF-TCNQ is characteristic of a three-dimensional to one-dimensional mean-field-theory crossover<sup>19,48</sup> and most probably arises from fitting the experimental data outside of the region of asymptotic three-dimensional exponents. Therefore, it appears that TSeF-TCNQ has a comparatively smaller asymptotic three-dimensional region suggesting that the fluctuation growth in this material is slightly more anisotropic than in TTF-TCNQ.<sup>37</sup>

The below- $T_c$  analysis is further complicated by the existence in these materials of two distinct conducting chains.<sup>10</sup> The formalism discussed above must be generalized to allow for two coupled, complex order parameters, one for each chain. If the order parameters are linearly coupled, the critical behavior in the resistivity should be ade-

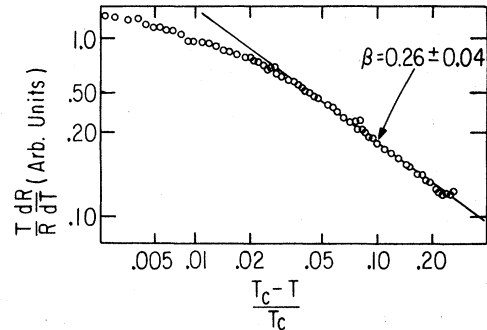


FIG. 9. Critical exponent for  $T < T_c$  of  $(1/R)(dR/dT)$ , where  $R$  is the  $b$ -axis resistance of TSeF-TCNQ.

quately described by the single chain model given above.<sup>49</sup> In such a model, the critical temperature dependence for  $T < T_c$  of the  $a$ - and  $b$ -axis resistivities would be identical. However, in the temperature range where the electronic gaps are large compared to  $k_B T$ , then even if the order parameters are linearly coupled, the  $a$ - and  $b$ -axis resistivities will in general have different temperature dependences.

Related to the coupled order parameter problem is the existence in TTF-TCNQ of a second phase transition at a temperature  $T'$ ; where experimentally  $46 \lesssim T' \lesssim 48$  K.<sup>8,49</sup> We will not discuss this transition here except to say that the validity of Eq. (5.3) is obviously limited to  $T > T'$ . An analysis of the critical behavior in the  $a$ -axis resistivity of TTF-TCNQ for  $T < T_c$  has been frustrated by the large degree of broadening of the transition in the samples studied and by the near proximity of the transition at  $T'$ . The most definite statement we can make at this time is that the behavior of the  $a$ -axis resistivity for  $T < T_c$  is qualitatively similar to the  $b$ -axis behavior as  $T - T_c \rightarrow 0^-$ . Even without quantitative critical-exponent measurements for  $T < T_c$ , the qualitative agreement of the low-temperature data with the predictions of Eqs. (4.13) and (4.14) gives strong independent confirmation of our conclusion that short-range one-dimension-

al order is not well developed for  $T > T_c$ . Continued work on this problem is presently underway.

In conclusion, our experimental results suggest that the conductivity above  $T_c$  in both TTF-TCNQ and TSeF-TCNQ is dominated by an anomaly in the electron-phonon scattering associated with the onset of a three-dimensional Peierls distortion. Below  $T_c$  the critical behavior in the conductivity appears to be dominated by the opening of an electronic gap at the Fermi surface and is consistent with the notion that the fluctuation growth in these materials is far more isotropic than one would expect given the anisotropy in the conductivity. Finally, it is difficult to reconcile these results with arguments that suggest the existence of a well-defined (i.e., width  $\ll k_B T$ ) collective mode at room temperature<sup>11,13</sup> since the sharp critical behavior in the resistivity suggests that relatively long-range one-dimensional order is not established even at much lower temperatures.

The authors would like to thank the scientists listed in Ref. 20 for providing the samples used in this study and Marshall Cohen and A. J. Heeger for providing us with numerical values of published  $a$ -axis resistivity data.<sup>12</sup> Special thanks are due to M. H. Cohen, A. J. Hertz, and G. Mazenko for many stimulating discussions.

\*Work supported by NSF under contract No. NSF-DMR75-14360 and by the Louis B. Block Fund of the University of Chicago. We have also benefited from support of the Materials Research Laboratory of the NSF.

†Supported in part by the Alfred P. Sloan Research Foundation.

<sup>1</sup>F. Denoyer, R. Comes, A. F. Garito, and A. J. Heeger, *Phys. Rev. Lett.* **35**, 445 (1975).

<sup>2</sup>S. Kagoshima, H. Anzai, K. Kajimura, and T. Ishigoro, *J. Phys. Soc. Jpn.* **39**, 1143 (1975).

<sup>3</sup>R. Comes, S. M. Shapiro, G. Shirane, A. F. Garito, and A. J. Heeger, *Phys. Rev. Lett.* **35**, 1518 (1975); *Phys. Rev. B* (to be published).

<sup>4</sup>H. A. Mook and C. R. Watson, *Phys. Rev. Lett.* **36**, 801 (1976).

<sup>5</sup>J. H. Perlstein, J. P. Ferraris, V. V. Walatka, and D. O. Cowan, *AIP Conf. Proc.* **10**, 1494 (1972); J. P. Ferraris, D. O. Cowan, V. V. Walatka, and J. H. Perlstein, *J. Am. Chem. Soc.* **95**, 948 (1973).

<sup>6</sup>L. B. Coleman, M. J. Cohen, D. J. Sandman, F. G. Yamagishi, A. F. Garito, and A. J. Heeger, *Solid State Commun.* **12**, 1125 (1973).

<sup>7</sup>R. A. Craven, M. B. Salomon, C. De Pasquali, R. M. Herman, G. Stucky, and A. Schultz, *Phys. Rev. Lett.* **32**, 769 (1974).

<sup>8</sup>Per Bak and V. J. Emery, *Phys. Rev. Lett.* **36**, 978 (1976).

<sup>9</sup>V. J. Emery, *Phys. Rev. Lett.* **37**, 107 (1976).

<sup>10</sup>A. N. Bloch, J. P. Ferraris, D. O. Cowan, and T. O. Poehler, *Solid State Commun.* **13**, 753 (1973); Y. Tomkiewicz, A. R. Taranko, and J. B. Torrance, *Phys. Rev. Lett.* **36**, 751 (1976).

<sup>11</sup>Marshall J. Cohen, L. B. Coleman, A. F. Garito, and A. J. Heeger, *Phys. Rev. B* **13**, 5111 (1976), and references therein.

<sup>12</sup>M. J. Cohen, L. B. Coleman, A. F. Garito, and A. J. Heeger, *Phys. Rev. B* **10**, 1298 (1974).

<sup>13</sup>D. B. Tanner, C. S. Jacobsen, A. F. Garito, and A. J. Heeger, *Phys. Rev. Lett.* **32**, 1301 (1974); and C. S. Jacobsen, D. B. Tanner, A. F. Garito, and A. J. Heeger, *ibid.* **33**, 1559 (1974).

<sup>14</sup>S. K. Khanna, E. Ehrenfreund, A. F. Garito, and A. J. Heeger, *Phys. Rev. B* **10**, 2205 (1974).

<sup>15</sup>R. E. Peierls, *Quantum Theory of Solids* (Oxford U. P., London, 1955), p. 108.

<sup>16</sup>L. D. Landau and E. M. Lifshitz, *Statistical Physics* (Pergamon, London, 1958), p. 482.

<sup>17</sup>D. Kuse and H. R. Zeller, *Phys. Rev. Lett.* **27**, 1060 (1971).

<sup>18</sup>H. R. Zeller, in *Low-Dimensional Cooperative Phenomena*, edited by H. J. Keller (Plenum, New York, 1975), p. 215; P. Bruesch, S. Strassler, and H. R. Zeller, *Phys. Rev. B* **12**, 219 (1975).

<sup>19</sup>P. M. Horn and D. Rimai, *Phys. Rev. Lett.* **36**, 809 (1976).

- <sup>20</sup>TTF-TCNQ samples were obtained from M. Miles (Monsanto Corp.), A. J. Heeger and A. F. Garito (University of Pennsylvania), A. N. Bloch (The Johns Hopkins University), and G. A. Thomas and F. Wudl (Bell Telephone Laboratories). TSeF-TCNQ samples were obtained from E. Engler (IBM, Yorktown Heights).
- <sup>21</sup>D. E. Schafer, W. Wudl, G. A. Thomas, J. P. Ferraris, and D. O. Cowan, *Solid State Commun.* **14**, 347 (1974).
- <sup>22</sup>R. Groff, A. Suna, and R. Merrifield, *Phys. Rev. Lett.* **33**, 418 (1974); H. Kahlert, *Solid State Commun.* **17**, 1161 (1975).
- <sup>23</sup>S. Etemad, T. Penney, E. M. Engler, B. A. Scott, and P. E. Seiden, *Phys. Rev. Lett.* **34**, 741 (1975), and A. N. Bloch (private communication).
- <sup>24</sup>A. Madhukar and Morrel H. Cohen (unpublished).
- <sup>25</sup>P. E. Seiden and Dario Cabib, *Phys. Rev. B* **13**, 1846 (1976).
- <sup>26</sup>See, for example, R. A. Craven and R. D. Parks, *Phys. Rev. Lett.* **31**, 383 (1973).
- <sup>27</sup>G. T. Meaden, N. H. Sze, and J. R. Johnston, in *Dynamical Aspects of Critical Phenomena*, edited by J. I. Budnick and M. P. Kawatra (Gordon and Breach, New York, 1972), p. 315.
- <sup>28</sup>M. E. Fisher and J. S. Langer, *Phys. Rev. Lett.* **20**, 665 (1968).
- <sup>29</sup>Y. Suezaki and H. Mori, *Prog. Theor. Phys.* **41**, 1177 (1969); also, see, S. Takada, *Prog. Theor. Phys.* **46**, 15 (1971).
- <sup>30</sup>T. Kasuya and A. Kondo, *Solid State Commun.* **14**, 249 (1974).
- <sup>31</sup>I. Mannari, *Phys. Lett.* **26A**, 134 (1968).
- <sup>32</sup>J. Bardeen, *Solid State Commun.* **13**, 357 (1973); D. Allender, J. W. Bray, and J. Bardeen, *Phys. Rev. B* **9**, 119 (1974).
- <sup>33</sup>B. R. Patton and L. J. Sham, *Phys. Rev. Lett.* **33**, 638 (1974); P. F. Maldague and B. R. Patton (unpublished).
- <sup>34</sup>P. A. Lee, T. M. Rice, and P. W. Anderson, *Phys. Rev. Lett.* **31**, 462 (1973); *Solid State Commun.* **14**, 703 (1974).
- <sup>35</sup>David Pines and Philippe Nozières, *The Theory of Quantum Liquids* (Benjamin, New York, 1966), p. 85.
- <sup>36</sup>See, for example, S. K. Ma, *Modern Theory of Critical Phenomena* (Benjamin, New York, 1976); and R. Brout, *Phase Transitions* (Benjamin, New York, 1965).
- <sup>37</sup>D. J. Scalapino, Y. Imry, and P. Pincus, *Phys. Rev. B* **11**, 2042 (1975).
- <sup>38</sup>We assume a two-component order parameter.
- <sup>39</sup>J. C. Scott, A. F. Garito, and A. J. Heeger, *Phys. Rev. B* **10**, 3131 (1974); Y. Tomkiewicz, Y. B. Scott, L. J. Tao and R. S. Title, *Phys. Rev. Lett.* **30**, 1369 (1974).
- <sup>40</sup>The possibility of a spin-Peierls transition is not totally out of the question [J. B. Torrance (private communication)].
- <sup>41</sup>D. J. Scalapino, M. Sears, and R. A. Ferrell, *Phys. Rev. B* **6**, 3409 (1972).
- <sup>42</sup>The absence of a well-defined peak in the specific heat in Ref. 41 results from neglecting weakly-temperature-dependent prefactors [D. J. Scalapino and B. Stoeckly (private communication)].
- <sup>43</sup>A. J. Berlinsky, J. F. Carolan, and L. Weiler, *Solid State Commun.* **15**, 795 (1974); also see Ref. 7.
- <sup>44</sup>A. A. Bright, A. F. Garito, and A. J. Heeger, *Solid State Commun.* **13**, 943 (1973); *Phys. Rev. B* **10**, 1328 (1974).
- <sup>45</sup>B. Horovitz, H. Gutfreund, and M. Wegner, *Phys. Rev. B* **12**, 3174 (1975).
- <sup>46</sup>J. C. Phillips (unpublished).
- <sup>47</sup>The more correct form which includes weakly-temperature-dependent prefactors is  $(T/R)(dR/dT) \sim (-t)^{\beta-1}$ . When absolute  $T$  changes substantially over the region of fit (as in Fig. 9) the extra factor of  $T$  must be included.
- <sup>48</sup>R. J. Birgeneau, G. Shirane, and T. A. Kitchens, in *Proceedings of the Thirteenth International Conference on Low Temperature Physics* (Plenum, New York, 1972), p. 371.
- <sup>49</sup>R. A. Craven, S. Etemad, T. Penney, P. M. Horn, and D. Guidotti (unpublished).